Journal of Materials Chemistry B

Accepted Manuscript

ROYAL SOCIETY OF CHEMISTRY

www.rsc.org/materialsB

Table of Contents (TOC) Image

Dendrimer-functionalized electrospun cellulose acetate nanofibers for targeted cancer cell capture applications†

Yili Zhao,[ab] Xiaoyue Zhu,[c] Hui Liu,[c] Yu Luo,[c] Shige Wang,[a] Mingwu Shen,[c] Meifang Zhu,[a] Xiangyang Shi*[ac]

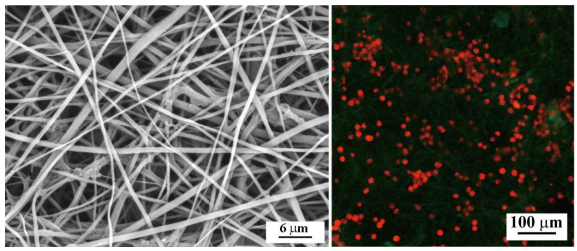

Multifunctional folic acid-functionalized dendrimers can be modified onto the surface of electrospun cellulose acetate nanofibers for specific capture of FAR-overexpressing cancer cells.

Journal of
Materials Chemistry B

Cite this: DOI: 10.1039/c0xx00000x

PAPER

www.rsc.org/xxxxxx

Dendrimer-functionalized electrospun cellulose acetate nanofibers for targeted cancer cell capture applications†

Yili Zhao,[ab] Xiaoyue Zhu,[c] Hui Liu,[c] Yu Luo,[c] Shige Wang,[a] Mingwu Shen,[c] Meifang Zhu,[a] Xiangyang Shi*[ac]

Received (in XXX, XXX) Xth XXXXXXXXX 20XX, Accepted Xth XXXXXXXXX 20XX
DOI: 10.1039/b000000x

Cancer cell metastasis causes 90% of cancer patient death. Detection and targeted capture of cancer cells *in vitro* is of paramount importance. Development of novel nanodevices for cancer cell capture applications, however, still remains a great challenge. Here we report a facile approach to fabricating multifunctional dendrimer-modified electrospun cellulose acetate (CA) nanofibers for targeted cancer cell capture applications. In this study, hydrolyzed electrospun CA nanofibers with negative surface charge were layer-by-layer assembled with a bilayer of poly(diallyldimethylammonium chloride) (PDADMAC) and polyacrylic acid (PAA) *via* electrostatic interaction. Thereafter, amine-terminated generation 5 poly(amidoamine) dendrimers pre-modified with folic acid (FA) and fluorescein isothiocyanate were covalently conjugated onto the bilayer-assembled nanofibers *via* 1-ethyl-3-(3-dimethylaminopropyl) carbodiimide hydrochloride coupling reaction, followed by acetylation to neutralize the remaining dendrimer surface amines. The formation of electrospun CA nanofibers, assembly of PDADMAC/PAA bilayer onto the CA nanofibers, and the dendrimer modification onto the nanofibers were characterized *via* different techniques. The formed dendrimer-modified CA nanofibers were then used to capture cancer cells overexpressing FA receptors. We show that the bilayer self-assembly and the subsequent dendrimer modification does not appreciably change the fiber morphology. Importantly, the modification of FA-targeted multifunctional dendrimers renders the CA nanofibers with superior capability to specifically capture cancer cells (KB cells, a model cancer cell line) overexpressing high-affinity FA receptors. The approach to modifying electrospun nanofibers with multifunctional dendrimers may be extended to fabricate other functional nanodevices for capturing different types of cancer cells.

Introduction

Dividing and growing uncontrollably, cancer cells invade nearby organs, or spread to distant parts of the body through lymphatic system or bloodstream to form malignant tumors.[1] At present, metastasis is the main reason for cancer-related death.[2] Capturing circulating tumor cells, which escape from the primary tumor and invade into the lymphatic system or bloodstream, plays a significant role in the early detection of potential fatal metastases.[3]

Development of cancer cell capturing technology has witnessed a tremendous progress in recent years. Various technologies have been established to capture cancer cells that circulate in the bloodstream, such as immunomagnetic separation,[4] size-selective microcavity,[3] micropost technology,[5-7] and nanostructure-based systems.[8-13] Among these methods, nanostructure-based nanodevices have been recognized as one of the simplest and most efficient methods for cancer cell capturing applications. In particular, electrospun nanofibers produced *via* a simple and versatile electrospinning technology display similar dimensions to the cellular surface components (e.g., microvilli and filopodia) and extracellular matrix (ECM),[13] can provide sufficient space for cell attachment and proliferation due to their large surface-to-volume ratio and high porosity.[14] Importantly, the fiber surfaces can be easily modified to have multifunctionality.[15] A variety of materials including naturally occurring[16-18] and synthetic polymers,[14, 19-22] ceramics and metals,[23, 24] or the mixture of them[25-29] have been used to fabricate nanofibers with controllable dimension and morphology. Therefore, electrospun nanofibers have been of paramount importance to develop nanodevices for capturing of cancer cells.

To render the nanofibers with cell capturing capability, a variety of cell specific bioactive ligands including antibody,[12] polypeptide,[30] and E-selectin[31] have been immobilized onto the surface of nanofibers. In general, nanofibers can be surface functionalized *via* different approaches including but not limited to layer-by-layer assembly,[32-34] plasma treatment,[35] wet chemical method,[36] and co-electrospinning of bioactive molecules and polymers.[17, 37] Our previous work has shown that electrospun nanofibers can be functionalized through the use of dendrimers as

a crosslinker[38] or through dendrimer-mediated assembly.[39]

Dendrimers are a family of highly branched, monodispersed, synthetic macromolecules with well defined structure and composition.[40] The unique structural property of dendrimers affords their uses as multifunctional nanoplatforms to be modified with targeting ligands, drug molecules, and imaging agents for different nanomedicinal applications.[41-45] For instance, dendrimers can be linked with a variety of targeting ligands such as folic acid (FA),[46, 47] arginine-glycine-aspartic acid peptide,[48-50] and lactobionic acid (LA)[51, 52] *via* covalent bonding for specific targeted detection of cancer cells. Alternatively, functionalized dendrimers can be modified or assembled onto other nano-objects for targeted cancer imaging and therapy.[53-55] These prior successes in the dendrimer chemistry for nanomedicinal applications and in the surface modification of electrospun nanofibers lead us to hypothesize that multifunctional targeting ligand-modified dendrimers may also be covalently modified onto the surface of electrospun nanofibers for cancer cell capture applications.

In this present study, we developed a facile approach to modifying multifunctional amine-terminated fluorescein isothiocyanate (FI)- and FA-modified generation 5 poly(amidoamine) (PAMAM) dendrimers (G5.NH_2-FI-FA) onto electrospun cellulose acetate (CA) nanofibers. Electrospun CA nanofibers were first hydrolyzed to render their surfaces with negative charge, then assembled with a bilayer of poly(diallyldimethylammonium chloride) (PDADMAC) and polyacrylic acid (PAA) *via* electrostatic layer-by-layer (LbL) deposition, followed by modification with G5.NH_2-FI-FA dendrimers *via* 1-ethyl-3-[3-dimethylaminopropyl] carbodiimide hydrochloride (EDC) reaction. The remaining dendrimer terminal amines were then acetylated to avoid the non-specific binding of the fibrous mat with negatively charged cell membranes (Scheme 1). The formed dendrimer-functionalized CA nanofibrous mats were characterized *via* different techniques. Then the dendrimer-functionalized CA nanofibrous mats were used to specifically capture cancer cells overexpressing FA receptors (FAR). To our knowledge, this is the first report related to the use of dendrimer-functionalized electrospun nanofibers for specific cancer cell capturing applications.

Experimental

Materials

CA (Mw = 30,000, 39.8 wt% acetyl groups), PAA (average Mw = 240,000, 25 wt% in water), PDADMAC (average Mw = 100,000-200,000, 20 wt% in water), FA, FI, EDC, triethylamine, propidium iodide (PI), and acetic anhydride were supplied by Sigma-Aldrich (St. Louis, MO). G5.NH_2 PAMAM dendrimers were purchased from Dendritech (Midland, MI). Acetone, N,N-dimethylformamide, and all other chemicals and solvents were acquired from Sinopharm Chemical Reagent Co., Ltd. (Shanghai, China). KB cells (a human epithelial carcinoma cell line) and L929 cells (a mouse fibroblast cell line) were obtained from Institute of Biochemistry and Cell Biology (the Chinese Academy of Sciences, Shanghai, China). RPMI 1640 medium, Dulbecco's Modified Eagle's medium (DMEM), fetal bovine serum (FBS), penicillin, and streptomycin were from Hangzhou Jinuo Biomedical Technology (Hangzhou, China). Water used in all experiments was purified using a Milli-Q Plus 185 water purification system (Millipore, Bedford, MA) with a resistivity higher than 18.2 MΩ·cm. Regenerated cellulose dialysis membranes with molecular weight cut-off (MWCO) at 14,000 were acquired from Fisher (Pittsburgh, PA).

Synthesis of G5.NH_2-FI-FA conjugate

G5.NH_2 dendrimer was sequentially modified with FI and FA according to our previous reports.[44, 56, 57] Briefly, a dimethyl sulfoxide (DMSO) solution of FI (12.8 μmol, 1.465 mL) was added into a DMSO solution of G5.NH_2 (2.56 μmol, 6.647 mL) under vigorous magnetic stirring at room temperature. After 24 h, the raw product of G5.NH_2-FI conjugate in the DMSO solution was added with a DMSO solution (6.6 mL) of FA (12.8 μmol, 5 mL) activated by EDC (64.0 μmol, 1.60 mL) at room temperature for 3 h. The reaction mixture was stirred for 3 days, followed by dialysis against phosphate buffered saline (PBS, 3 times, 2 L) and water (6 times, 2 L) for 3 days. Then, the dialysis liquid was lyophilized to obtain the G5.NH_2-FI-FA conjugate.

The control G5.NH_2-FI conjugate without FA conjugation was synthesized according to the same procedure described above. A DMSO solution of FI (12.78 μmol, 1.58 mL) was added into a DMSO solution of G5.NH_2 dendrimer (2.556 μmol, 6.649 mL) under magnetic stirring. After 24 h, the reaction mixture was subjected to dialysis and lyophilization according to the above protocols to obtain the G5.NH_2-FI conjugate.

Fabrication of electrospun CA nanofibers

Electrospun CA nanofibers were fabricated according to protocols described in our previous reports.[32, 34] In brief, CA powder (3.0 g) was dissolved into a mixed solvent of acetone/N,N-dimethylformamide (15 mL, v/v = 2:1) with continuous stirring until a clear and homogeneous solution was obtained. Freshly prepared CA solution was loaded into a syringe with a needle having an inner diameter of 0.8 mm. The feeding rate was controlled to be 1.0 mL/h by a syringe pump. The electrical potential was fixed at 21 kV, and the tip to collector distance was set at 25 cm. The electrospinning process was carried out under ambient conditions (humidity, 40-50 %; temperature, 20-25 °C). The formed CA nanofibrous mats were dried in a vacuum oven for 24 h in order to remove the residual organic solvent and moisture.

Preparation of dendrimer-functionalized CA nanofibrous mats

CA nanofibers were first hydrolyzed to render them with negative surface charge according to the literature.[58, 59] A dried CA nanofibrous mat (e.g., 2.4 cm × 2.4 cm, 9.58 mg) was immersed into an ethanol solution of NaOH (0.05 M) for 4 h at room temperature, followed by rinsing with copious water.

The formed negatively charged CA nanofibrous mat was then assembled with PDADMAC/PAA bilayer via electrostatic LbL assembly according to the literature.[32-34] Aqueous solutions of PDADMAC and PAA were separately prepared to have a concentration of 2 mg/mL in 0.5 M NaCl, and the solution pH of both polymers was adjusted to 3.5 using 1 M HCl or 1 M NaOH. Then, a circular CA nanofibrous mat (203.90 mg with a diameter of 12.5 cm) was exposed to PDADMAC solution for 5 min,

rinsed with water for 3 times (2 min each time). After that, the PDADMAC-assembled CA mat was exposed to PAA solution for 5 min, and rinsed with water according to the above protocol. Thereafter, the formed PDADMAC/PAA-assembled CA nanofibrous mat was dried for at least 2 days in vacuum at ambient temperature prior to subsequent modification with dendrimers.

To modify dendrimers onto the surface of PDADMAC/PAA-assembled CA nanofibrous mat, a circular mat (diameter = 14 mm, 2.56 mg) was first exposed to an EDC solution (44.55 μmol, in 0.427 mL water) under gentle shaking for 3 h to activate the PAA carboxyl groups. Then, an aqueous G5.NH_2-FI-FA solution (0.427 mL, 2 mg/mL) was added into the suspension of PDADMAC/PAA-assembled CA mat with PAA surface groups activated and the suspension was shaken at room temperature for 3 days. The final concentrations of G5.NH_2-FI-FA and fiber mat were set at 1 and 3 mg/mL (as an example), respectively. To achieve the optimum modification of dendrimers onto the surface of PDADMAC/PAA-assembled CA nanofibrous mat, G5.NH_2-FI-FA with a final concentration at 0.2, 0.4, 0.6, 0.8, and 1.2 mg/mL, respectively was also used and a final nanofiber concentration was fixed at 3 mg/mL. To determine the dendrimer modification efficiency, the supernatants after G5.NH_2-FI-FA modification and rinsing with water were collected and quantified using Lambda 25 UV-vis spectrophotometer (Perkin Elmer, Boston, MA) at 500 nm according to the standard G5.NH_2-FI-FA concentration/absorbance calibration curve. To neutralize the remaining amines of dendrimers modified onto the fibrous mat, triethylamine with 5 molar equivalents of the dendrimer surface amines was added to the aqueous suspension of the dendrimer-functionalized CA nanofibrous mat under gentle shaking for 30 min. Then, acetic anhydride with similar molar equivalents of triethylamine was added and the suspension was shaken for 24 h. Thereafter, the nanofibrous mat was thoroughly rinsed with water and dried in a vacuum oven for at least 24 h to obtain G5.NHAc-FI-FA-modified CA nanofibrous mat. For comparison, PDADMAC/PAA-assembled CA nanofibrous mat was also modified with G5.NH_2-FI conjugate to form G5.NHAc-FI-modified CA nanofibrous mat according to the optimized G5.NH_2-FI-FA dendrimer concentration under similar experimental conditions.

Characterization

^{1}H NMR spectra of G5.NH_2-FI-FA or G5.NH_2-FI were recorded on a Bruker DRX 400 nuclear magnetic resonance spectrometer (Rheinstetten, Germany). Samples were dissolved in D_2O before measurements. Morphology of the CA nanofibers and G5.NHAc-FI-FA- or G5.NHAc-FI-modified CA nanofibrous mats was observed by scanning electron microscopy (SEM, JEOL JSM-5600LV, Japan) at an operating voltage of 10 kV. The samples were sputter coated with a 10 nm thick gold film before measurements. For each sample, 300 nanofibers from different images were randomly selected to analyze the fiber diameter distribution using Image J 1.40G software (http://rsb.info.nih.gov/ij/down-load.html). Fourier transform infrared spectroscopy (FTIR) was performed on a Nicolet Nexus 670 FTIR spectrometer using a transmission mode with a wavenumber range of 400-4000 cm^{-1}. The fluorescence property of the nanofibers after surface modification was characterized by confocal laser scanning microscope (CLSM, Carl Zeiss LSM700, Jena, Germany). The electrospun CA nanofibers were directly collected onto coverslips, modified according to the protocols described above, and then imaged using a 40 × objective lens.

Cell capture assay

KB cells and L929 cells were regularly cultured and passaged in 25 cm^2 tissue culture flasks with 5 mL 1640 medium and DMEM medium, respectively supplemented with penicillin (100 units/mL), streptomycin (100 μg/mL), and 10% heat-inactivated FBS at 37 °C and 5% CO_2. The KB cells grown in FA-free medium express high-level FAR (denoted as KB-HFAR), while the cells grown in FA-containing medium ([FA] = 2.5 μM) express low-level FAR (denoted as KB-LFAR).[47]

Dendrimer-modified CA fibrous mats with a circular shape (diameter = 14 mm) were placed onto cover slips with a similar diameter, and fixed in a 24-well plate using stainless steel rings. All the samples prepared in quadruplicate were sterilized under ultraviolet light irradiation for 2 h. Prior to cell seeding, the dendrimer (G5.NHAc-FI-FA or G5.NHAc-FI)-modified CA nanofibrous mats were incubated with cell culture medium overnight. Then, KB-HFAR cells were seeded onto the 24-well plate at a density of 5×10^4 cells/well and incubated at 37 °C, 5 % CO_2, and 95 % relative humidity for 10, 20, 40, and 60 min, respectively. The medium volume for cell seeding was 400 μL/well. At each pre-determined time point, the cell culture medium containing suspended cells was collected, and the cells attached onto the substrates were washed with PBS for 3 times. Then, the PBS washing solutions were merged with the collected cell suspension, followed by counting the number of cells using Scepter 2.0 Handheld Automated Cell Counter (Merck Millipore, Merck KGaA, Damstadt, Germany). The cell capture efficiency was calculated according to equation (1):

$$\text{Cell capture efficiency} = (n_0\text{-}n_t/n_0) \times 100\% \quad (1)$$

Where n_0 is the total number of cells before cell seeding, n_t is the number of cells in the cell suspension in combination with the PBS washing solutions. To further prove the targeted cancer cell capture ability, L929 cells and KB-LFAR cells were also seeded onto the targeted and non-targeted CA nanofibrous mats, treated, and analyzed under similar experimental conditions.

Confocal microscopy

The cancer cell capture ability of dendrimer-modified CA mats was also confirmed by confocal microscopy. In brief, KB-HFAR cells were seeded into each well pre-fixed with dendrimer-modified CA nanofibrous mats at a density of 5×10^4 cells/well with 1 mL RPMI 1640 medium and cultured at 37 °C and 5% CO_2 for 10, 20, 40, and 60 min, respectively. The cells were then washed 3 times with PBS, fixed with glutaraldehyde (2.5 %) at 4 °C for 15 min, and stained with PI (1 mg/mL, 20 μL) at 37 °C for 15 min using a standard procedure. The cells attached onto the nanofibrous mats were imaged using a 10× objective lens. For comparison, L929 cells cultured using DMEM were treated and observed under similar conditions.

Statistical analysis

One-way ANOVA statistical analysis was performed to compare the cell capture efficiency of the FA-targeted and non-targeted multifunctional dendrimer-modified nanofibrous mats. 0.05 was

selected as the significance level, and the data were indicated with (*) for $p < 0.05$, (**) for $p < 0.01$, and (***) for $p < 0.001$, respectively.

Results and discussion

Characterization of G5.NH_2-FI-FA dendrimers

Before modification of functionalized dendrimers onto the surface of CA nanofibers, multifunctional amine-terminated FI- and FA-modified G5 dendrimers (G5.NH_2-FI-FA) were synthesized according to protocols described in our previous work (Scheme 1a).[44, 53, 54, 56] The synthesized G5.NH_2-FI-FA conjugate was characterized by ^{1}H NMR spectroscopy (Figure 1). It can be seen that the peaks between 2 and 3.4 ppm are assigned to the –CH_2– protons of the G5 dendrimers, the peaks at 6.6, 7.5, and 8.5 ppm are assigned to the characteristic protons of the attached FA moiety. Likewise, the featured proton peaks at 6.4 and 7.0 ppm are assigned to the attached FI moiety. Based on NMR integration, the number of FA and FI moieties attached onto each dendrimer molecule was estimated to be 3.8 and 3.4, respectively (NMR intgration can be seen in Figure S1, electronic supplementary information, ESI). G5.NH_2-FI without FA conjugation was also synthesized and characterized by ^{1}H NMR spectroscopy (Figure S2, ESI). The number of FI moiety attached onto each G5 dendrimer was estimated to be 4.7. These NMR characterization results are consistent with those reported in our previous studies.[44, 47, 54, 60]

The synthesized G5.NH_2-FI-FA and G5.NH_2-FI conjugates were also characterized by UV-vis spectrometry (Figure S3, ESI). The characteristic absorption peak at 500 nm for both conjugates is associated with the attached FI moiety, suggesting the successful FI conjugation for both conjugates. As opposed to G5.NH_2-FI conjugate that does not display any apparent absorption features at 280 nm, the characteristic absorption peak of FA at 280 nm appearing in the UV-vis spectrum of G5.NH_2-FI-FA conjugate indicates the successful FA conjugation.

Fabrication and hydrolysis of electrospun CA nanofibers

Using a simple electrospinning technology under optimized conditions described in our previous work[32, 34],[32, 34] electrospun CA nanofibers were formed and characterized using SEM (Figure 2). It can be seen that smooth and continuous CA nanofibers with random orientation are able to be produced with a mean diameter of 431.6 ± 129.9 nm. The formed electrospun CA nanofibrous mats exhibit a three-dimensional porous structure, which is quite similar to ECM, in agreement with our previous report.[32]

To render the CA nanofibers with surface negative charge for subsequent self-assembly and dendrimer modification, the CA fibers were hydrolyzed in the presence of NaOH. The morphology of the CA nanofibers after hydrolysis at different time periods was observed by SEM (Figure S4, ESI). It can be seen that the porous and uniform fibrous structure of CA nnaofibers does not change significantly except that the surface of CA nanofibers becomes rough. After 8 h hydrolysis, some fibers began to break (Figure S4d). This may be due to the fact that the alkali saponification at a relatively long time likely transforms a high percentage of the CA acetyl groups to hydroxyl groups,[59] resulting in the structural destruction of the fibers. In order to hydrolyze the CA nanofibers as much as possible without changing their fibrous morphology, we selected 4 h as the optimum hydrolysis time.

FTIR spectroscopy was used to characterize the structure of the CA nanofibers before and after hydrolysis (Figure 3). The characteristic peaks at 1750, 1370, and 1235 cm^{-1} can be assigned to carbonyl stretching (νC=O), methyl bending (δC-CH_3), and alkoxyl stretching of the ester (νC-O-C), respectively, which represent the acetate substituent (Curve 2).[59] After hydrolysis, the decreased absorption intensity at 1750, 1370, and 1235 cm^{-1} related to the acetyl group content, the appearance of a new broad peak at 3400 cm^{-1} that can be assigned to the hydroxyl groups, and the absorption peak at 1160 cm^{-1} that can be assigned to the acetal linkages of the cellulose backbone suggest the successful partial hydrolysis of CA nanofibers (Curve 3).[61] Of particular interest, the peak at 1650 cm^{-1}, which belongs to the asymmetric stretching vibration of carboxylate (COO-) groups, increases after the hydrolysis of the CA nanofibers, in agreement with data reported in the literature.[62] FTIR results confirmed the structural transformation of CA nanofibers after hydrolysis to render them with negative surface charge.

Formation of multifunctional dendrimer-modified CA nanofibrous mats

The hydrolyzed CA nanofibrous mats were then assembled with one bilayer of PDADMAC/PAA *via* electrostatic LbL self-assembly, modified with G5.NH_2-FI-FA conjugate *via* EDC chemistry, followed by acetylation of the remaining dendrimer terminal amines (Scheme 1b). Our previous work has shown that deposition of more bilayers of PDADMAC/PAA onto CA nanofibers results in the pearl necklace like or ball-like structure of the CA fiber surface, or even block the pores of the fibrous mat,[34] therefore only one bilayer of PDADMAC/PAA was chosen to coat onto the hydrolyzed CA nanofibrous mats in this study. For comparison, non-targeted multifunctional dendrimer-modified nanofibrous mats (G5.NHAc-FI-modified CA nanofibers) were also prepared through a similar process.

The modification of the CA nanofibrous mats can be visually proven by the color change after the dendrimer modification step (Figure S5, ESI). It can be seen that in contrast to the hydrolyzed CA nanofibers with white color, the modification of both G5.NHAc-FI and G5.NHAc-FI-FA dendrimers renders the CA mats with light yellow color, which is associated with the color of the functionalized dendrimers. Furthermore, CLSM images of G5.NHAc-FI-FA dendrimer-functionalized CA nanofibers show that uniform FI-associated green fluorescence appears on the nanofiber surfaces (Figure 4), confirming the successful modification of dendrimers.

To ensure the maximum dendrimer modification onto the bilayer-assembled CA nanofibers, we used G5.NH_2-FI-FA dendrimers with different initial concentrations under a fixed nanofiber concentration of 3 mg/mL. The featured FI absorption at 500 nm allowed us to monitor the amount of dendrimers modified onto the nanofiber surfaces *via* UV-vis spectroscopy (Figure S6, ESI). It can be seen that with the increase of the initial G5.NH_2-FI-FA concentration, the difference of the FI absorbance at 500 nm before and after modification increases. At the G5.NH_2-FI-FA concentration of 1 mg/mL, the difference is the largest, suggesting the maximum dendrimer modification onto the fiber surfaces. As a result, we selected 1 mg/mL as the

optimum G5.NH_2-FI-FA concentration for further studies. Similarly, the concentration of the control dendrimer conjugate G5.NH_2-FI was also selected at 1 mg/mL. It can be seen from the UV-vis spectra of G5 dendrimers in aqueous solution before and after modification onto nanofibers (Figure S7, ESI), the absorbance of G5.NH_2-FI-FA or G5.NH_2-FI before modification was much higher than that after modification. This further demonstrated the successful dendrimer modification of the nanofibers. According to the calibration curve of G5.NH_2-FI-FA (Figure S7a) and G5.NH_2-FI (Figure S7c) at 500 nm, the amount of G5.NH_2-FI-FA and G5.NH_2-FI conjugate modified onto the fiber surfaces was calculated to be 0.056 and 0.043 mg/mg (fiber), respectively.

Figure 5 shows the SEM images of the G5.NHAc-FI-FA- and G5.NHAc-FI-modified CA nanofibers. It is obvious that the 3D porous structure of CA nanofibers does not appreciably change after the fiber surface assembly and dendrimer modification, except that the diameters of both fibers increase. The diameter of G5.NHAc-FI-FA- and G5.NHAc-FI-modified CA nanofibers was estimated to be 544.0 ± 198.9 and 506.9 ± 215.7 nm, respectively, which is larger than that of the pristine CA nanofibers before hydrolysis (431.6 ± 129.9 nm, Figure 2). The increased fiber diameter should be attributed to the swelling of the CA nanofibers during the process of hydrolysis[63, 64] and the subsequent fiber surface assembly with PDADMAC/PAA bilayer and modification with dendrimers.

FTIR spectroscopy was also used to confirm the modification of G5.NH_2-FI-FA and G5.NH_2-FI conjugates onto the surface of the PDADMAC/PAA bilayer-assembled nanofibers. As shown in Figure 3, the characteristic absorption peak of G5.NH_2 dendrimer at 1560 cm^{-1} (curve 1) can be detected after the modification of G5.NH_2-FI (curve 4) and G5.NH_2-FI-FA (curve 5) conjugates onto the surface of CA nanofibers, suggesting the successful formation of G5.NHAc-FI-FA- and G5.NHAc-FI-modified CA nanofibers.

Cell capture assay

We next evaluated the specific cancer cell capture ability of the G5.NHAc-FI-FA-modified CA nanofibrous mat. It is known that the modification of FA onto dendrimers is able to render the dendrimers with targeting specificity to cancer cells overexpressing FAR.[44, 46, 47, 53-56, 60, 65-67] It is expected that upon modification of FA-targeted dendrimers onto CA nanofibers, the nanofibers are able to capture FAR-overexpressing cancer cells *via* ligand-receptor interaction. The cell capture efficiency of G5.NHAc-FI-FA-modified CA nanofibrous mat at different time points was investigated (Figure 6). It can be seen that with the capture time, both G5.NHAc-FI-FA- and G5.NHAc-FI-modified CA mats have increased efficiency to capture KB-HFAR cells. At a given time point, the cell capture efficiency of G5.NHAc-FI-FA-modified CA mat is higher than that of the G5.NHAc-FI-modified CA mat without FA. Specifically the G5.NHAc-FI-FA-modified CA mat displays a cell capture efficiency of 36.3% and 82.7 % at 40 and 60 min, respectively, significantly higher than that of the control group ($p < 0.05$) with cell capture efficiencies of 19.2 % and 38.3 % at the corresponding time points. This highlights the role played by FA-mediated targeting that can render the G5.NHAc-FI-FA-modified CA mat with enhanced interaction with KB-HFAR cells *via* ligand-receptor interaction.

The specific cancer cell capture ability of the multifunctional dendrimer-modified nanofibers was also confirmed by confocal microscopic observation (Figure 7). In the confocal microscopic images, FI-associated green fluorescence of nanofibers due to the modification dendrimers and PI-labeled red fluorescent KB-HFAR cells can be clearly seen. Coinciding to the quantitative cell counting assay data (Figure 6), at a given time point, much more KB-HFAR cells can be captured onto the G5.NHAc-FI-FA-modified CA nanofibrous mat than onto G5.NHAc-FI-modified CA mat, especially at the time points of 40 and 60 min.

To further confirm the specificity of the G5.NHAc-FI-FA-modified CA mat to capture FAR-overexpressing cancer cells, normal L929 cells without FAR overexpression and KB-LFAR cells were studied (Figure 8). It is clear that the efficiencies to capture both L929 and KB-LFAR cells using FA-targeted CA mat are almost equivalent to those using the non-targeted CA mat at a given time point, indicating that the G5.NHAc-FI-FA-modified CA mat in this case does not show specificity to capture cells. The non-specific capture of L929 cells using both G5.NHAc-FI- and G5.NHAc-FI-FA-modified CA mats was also qualitatively confirmed by confocal microscopic observation (Figure S8, ESI). Apparently, both G5.NHAc-FI-FA- and G5.NHAc-FI-modified CA nanofibrous mats do not show specificity to capture L929 cells without FAR overexpression. The efficiency of the G5.NHAc-FI- and G5.NHAc-FI-FA-modified CA nanofibrous mats to capture KB-HFAR, L929, and KB-LFAR cells at different time points are summarized in Table S1 (ESI). Taken together, our results clearly suggest that G5.NHAc-FI-FA-modified CA mat displays specificity to capture FAR-overexpressing cancer cells *via* ligand-receptor interaction.

Conclusion

In summary, we develop a convenient approach to fabricating multifunctional dendrimer-modified nanofibrous mats for targeted cancer cell capture applications. Via simple self-assembly and EDC-mediated coupling chemistry, multifunctional FA-targeted G5 dendrimers are able to be modified onto the surface of CA nanofibers. The modification of FA-targeted G5 dendrimers renders the CA nanofibers with excellent specificity to capture FAR-overexpressing cancer cells via ligand-receptor interaction. This approach to modifying electrospun nanofibers may be extended to prepare other functional nanofiber systems for capturing different types of cancer cells, and may hold great promise to detect cancer cells in lymphatic system or bloodstream.

Acknowledgements

This research is financially supported by the High-Tech Research and Development Program of China (2012AA030309) and the Program for Professor of Special Appointment (Eastern Scholar) at Shanghai Institutions of Higher Learning. Y. Zhao thanks the Innovation Funds of Donghua University Doctorate Dissertation of Excellence (101-06-0019014).

Notes and references

[a] *State Key Laboratory for Modification of Chemical Fibers and Polymer Materials, College of Materials Science and Engineering, Donghua*

University, Shanghai 201620, People's Republic of China. E-mail: xshi@dhu.edu.cn
[b] College of Textiles, Donghua University, Shanghai 201620, People's Republic of China.
[c] College of Chemistry, Chemical Engineering and Biotechnology, Donghua University, Shanghai 201620, People's Republic of China.

† **Electronic supplementary information (ESI) available**: additional experimental results.

1. A. Mantovani, *Nature*, 2009, **457**, 36-37.
2. P. Mehlen and A. Puisieux, *Nat. Rev. Cancer*, 2006, **6**, 449-458.
3. M. Hosokawa, T. Hayata, Y. Fukuda, A. Arakaki, T. Yoshino, T. Tanaka and T. Matsunaga, *Anal. Chem.*, 2010, **82**, 6629-6635.
4. A. E. L. M. Hoeppener, J. F. Swennenhuis and L. W. M. M. Terstappen, in *Minimal residual disease and circulating tumor cells in breast cancer*, eds. M. Ignatiadis, C. Sotiriou and K. Pantel, Springer, Berlin, 2012, pp. 43-58.
5. L. Chen, X. L. Liu, B. Su, J. Li, L. Jiang, D. Han and S. T. Wang, *Adv. Mater.* , 2011, **23**, 4376-4380.
6. S. Hou, H. C. Zhao, L. B. Zhao, Q. L. Shen, K. S. Wei, D. Y. Suh, A. Nakao, M. A. Garcia, M. Song and T. Lee, *Adv. Mater.*, 2013, **25**, 1547-1551.
7. S. Nagrath, L. V. Sequist, S. Maheswaran, D. W. Bell, D. Irimia, L. Ulkus, M. R. Smith, E. L. Kwak, S. Digumarthy and A. Muzikansky, *Nature*, 2007, **450**, 1235-1239.
8. S. Hou, L. B. Zhao, Q. L. Shen, J. H. Yu, C. Ng, X. J. Kong, D. X. Wu, M. Song, X. H. Shi and X. C. Xu, *Angew. Chem. Int. Ed.*, 2013, **52**, 3379-3383.
9. S. H. Jun, K. Kim, H. J. An, B. C. Kim, C. H. Sonn, M. Kim, J. Doh, C. Yee, K. M. Lee and J. Kim, *Adv. Funct. Mater.*, 2012, **22**, 4448-4455.
10. Y. J. Kim, M. Ebara and T. Aoyagi, *Angew. Chem. Int. Ed.*, 2012, **124**, 10689-10693.
11. Y. L. Luo, S. Nartker, H. Miller, D. Hochhalter, M. Wiederoder, S. Wiederoder, E. Setterington, L. T. Drzal and E. C. Alocilja, *Biosens. Bioelectron.*, 2010, **26**, 1612-1617.
12. Z. B. Zha, C. Cohn, Z. F. Dai, W. G. Qiu, J. H. Zhang and X. Y. Wu, *Adv. Mater.*, 2011, **23**, 3435-3440.
13. N. G. Zhang, Y. L. Deng, Q. D. Tai, B. Cheng, L. B. Zhao, Q. L. Shen, R. X. He, L. Y. Hong, W. Liu and S. S. Guo, *Adv. Mater.*, 2012, **24**, 2756-2760.
14. R. L. Qi, X. Y. Cao, M. W. Shen, R. Guo, J. Y. Yu and X. Y. Shi, *J. Biomater. Sci. Polym. Ed.*, 2012, **23**, 299-313.
15. C. P. Barnes, S. A. Sell, E. D. Boland, D. G. Simpson and G. L. Bowlin, *Adv. Drug Deliv. Rev.*, 2007, **59**, 1413-1433.
16. M. Y. Li, M. J. Mondrinos, M. R. Gandhi, F. K. Ko, A. S. Weiss and P. I. Lelkes, *Biomaterials*, 2005, **26**, 5999-6008.
17. H. Liao, R. Qi, M. Shen, X. Cao, R. Guo, Y. Zhang and X. Shi, *Colloid Surf. B-Biointerfaces*, 2011, **84**, 528-535.
18. S. G. Wang, X. Y. Cao, M. W. Shen, R. Guo, I. Bányai and X. Y. Shi, *Colloid Surf. B-Biointerfaces*, 2012, **89**, 254-264.
19. S. Wang, F. Zheng, Y. Huang, Y. Fang, M. Shen, M. Zhu and X. Shi, *ACS Appl. Mater. Interfaces*, 2012, **4**, 6393-6401.
20. S. G. Wang, R. Castro, X. An, C. L. Song, Y. Luo, M. W. Shen, H. Tomás, M. F. Zhu and X. Y. Shi, *J. Mater. Chem.*, 2012, **22**, 23357-23367.
21. F. Y. Zheng, S. G. Wang, M. W. Shen, M. F. Zhu and X. Y. Shi, *Polym. Chem.*, 2013, **4**, 933-941.
22. F. Y. Zheng, S. G. Wang, S. H. Wen, M. W. Shen, M. F. Zhu and X. Y. Shi, *Biomaterials*, 2013, **34**, 1402-1412.
23. D. Li and Y. N. Xia, *Nano Lett.*, 2003, **3**, 555-560.
24. H. Wu, R. Zhang, X. X. Liu, D. D. Lin and W. Pan, *Chem. Mater.*, 2007, **19**, 3506-3511.
25. X. Fang, H. Ma, S. Xiao, M. Shen, R. Guo, X. Cao and X. Shi, *J. Mater. Chem.*, 2011, **21**, 4493-4501.
26. Y. Huang, H. Ma, S. Wang, M. Shen, R. Guo, X. Cao, M. Zhu and X. Shi, *ACS Appl. Mater. Interfaces*, 2012, **4**, 3054-3061.
27. H. Ma, Y. Huang, M. Shen, D. Hu, H. Yang, M. Zhu, S. Yang and X. Shi, *RSC Adv.*, 2013, **3**, 6455-6465.
28. S. Xiao, M. Shen, R. Guo, S. Wang and X. Shi, *J. Phys. Chem. C*, 2009, **113**, 18062-18068.
29. S. Xiao, M. Shen, H. Ma, X. Fang, Q. Huang, W. J. Weber, Jr. and X. Shi, *J. Nanosci. Nanotechnol.*, 2011, **11**, 5089-5097.
30. Y. Y. Wang, L. X. Lü, Z. Q. Feng, Z. D. Xiao and N. P. Huang, *Biomed. Mater.*, 2010, **5**, 1-9.
31. K. Ma, C. K. Chan, S. Liao, W. K. Hwang, Q. Feng and S. Ramakrishna, *Biomaterials*, 2008, **29**, 2096-2103.
32. Y. Luo, S. G. Wang, M. W. Shen, R. L. Qi, Y. Fang, R. Guo, H. D. Cai, X. Y. Cao, H. Tomás, M. F. Zhu and X. Shi, *Carbohydr. Polym.*, 2013, **91**, 419-427.
33. T. Ogawa, B. Ding, Y. Sone and S. Shiratori, *Nanotechnology*, 2007, **18**, 1-8.
34. S. L. Xiao, S. Q. Wu, M. W. Shen, R. Guo, Q. G. Huang, S. Y. Wang and X. Y. Shi, *ACS Appl. Mater. Interfaces*, 2009, **1**, 2848-2855.
35. T. Desmet, R. Morent, N. D. Geyter, C. Leys, E. Schacht and P. Dubruel, *Biomacromolecules*, 2009, **10**, 2351-2378.
36. X. Lu, C. Wang and Y. Wei, *Small*, 2009, **5**, 2349-2370.
37. Y. K. Luu, K. Kim, B. S. Hsiao, B. Chu and M. Hadjiargyrou, *J. Controlled Release*, 2003, **89**, 341-353.
38. S. Wang, J. Zhu, M. Shen, M. Zhu and X. Shi, *ACS Appl. Mater. Interfaces*, 2014, **6**, 2153-2161.
39. D. Hu, Y. Huang, H. Liu, H. Wang, S. Wang, M. Shen, M. Zhu and X. Shi, *J. Mater. Chem. A*, 2014, **2**, 2323-2332.
40. D. A. Tomalia and J. M. J. Frechet, *Dendrimers and Other Dendritic Polymers*, John Wiley & Sons Ltd, New York, 2001.
41. Q. Chen, K. Li, S. Wen, H. Liu, C. Peng, H. Cai, M. Shen, G. Zhang and X. Shi, *Biomaterials*, 2013, **34**, 5200-5209.
42. I. J. Majoros, A. Myc, T. Thomas, C. B. Mehta and J. R. Baker, *Biomacromolecules*, 2006, **7**, 572-579.
43. C. Peng, L. Zheng, Q. Chen, M. Shen, R. Guo, H. Wang, X. Cao, G. Zhang and X. Shi, *Biomaterials*, 2012, **33**, 1107-1119.
44. Y. Wang, R. Guo, X. Y. Cao, M. W. Shen and X. Y. Shi, *Biomaterials*, 2011, **32**, 3322-3329.
45. S. Wen, K. Li, H. Cai, Q. Chen, M. Shen, Y. Huang, C. Peng, W. Hou, M. Zhu, G. Zhang and X. Shi, *Biomaterials*, 2013, **34**, 1570-1580.
46. X. Y. Shi, S. H. Wang, S. Meshinchi, M. E. Van Antwerp, X. D. Bi, I. Lee and J. R. Baker, *Small*, 2007, **3**, 1245-1252.
47. X. Y. Shi, S. H. Wang, M. E. Van, X. S. Chen and J. R. Baker, *Analyst*, 2009, **134**, 1373-1379.
48. E. Hill, R. Shukla, S. S. Park and J. R. Baker, Jr., *Bioconjugate Chem.*, 2007, **18**, 1756-1762.
49. Z. M. Li, P. Huang, X. J. Zhang, J. Lin, S. Yang, B. Liu, F. Gao, P. Xi, Q. S. Ren and D. X. Cui, *Mol. Pharmaceutics*, 2010, **7**, 94-104.
50. S. J. Zhu, L. L. Qian, M. H. Hong, L. H. Zhang, Y. Y. Pei and Y. Y. Jiang, *Adv. Mater.*, 2011, **23**, H84-H89.
51. R. Guo, Y. Yao, G. C. Cheng, S. H. Wang, Y. Li, M. W. Shen, Y. H. Zhang, J. R. Baker, Jr., J. H. Wang and X. Y. Shi, *RSC Adv.*, 2012, **2**, 99-102.
52. H. Liu, H. Wang, Y. Xu, R. Guo, S. Wen, Y. Huang, W. Liu, M. Shen, J. Zhao, G. Zhang and X. Shi, *ACS Appl. Mater. Interfaces*, 2014, **6**, 6944-6953.
53. X. Shi, S. H. Wang, S. D. Swanson, S. Ge, Z. Cao, M. E. Van Antwerp, K. J. Landmark and J. R. Baker, *Adv. Mater.*, 2008, **20**, 1671-1678.
54. S. H. Wang, X. Shi, M. Van Antwerp, Z. Cao, S. D. Swanson, X. Bi and J. R. Baker, *Adv. Funct. Mater.*, 2007, **17**, 3043-3050.
55. S. Wen, H. Liu, H. Cai, M. Shen and X. Shi, *Adv. Healthcare Mater.*, 2013, **2**, 1267-1276.
56. Y. Wang, X. Cao, R. Guo, M. Shen, M. Zhang, M. Zhu and X. Shi, *Polym. Chem.*, 2011, **2**, 1754-1760.
57. M. E. Zhang, R. Guo, Y. Wang, X. Y. Cao, M. W. Shen and X. Y. Shi, *Int. J. Nanomed.*, 2011, **6**, 2337-2349.
58. B. Ding, J. Du and Y. L. Hsieh, *J. Appl. Polym. Sci.*, 2011, **121**, 2526-2534.
59. K. Rodríguez, S. Renneckar and P. Gatenholm, *ACS Appl. Mater. Interfaces*, 2011, **3**, 681-689.
60. T. Y. Xiao, W. X. Hou, X. Y. Cao, S. H. Wen, M. W. Shen and X. Y. Shi, *Biomater. Sci.*, 2013, **1**, 1172-1180.

61. H. Q. Liu and Y. L. Hsieh, *J. Polym. Sci. Pt. B-Polym. Phys.*, 2002, **40**, 2119-2129.
62. S. H. Chen and K. Kimura, *Langmuir*, 1999, **15**, 1075-1082.
63. K. Abe, S. Iwamoto and H. Yano, *Biomacromolecules*, 2007, **8**, 3276-3278.
64. C. Y. Tang and H. Q. Liu, *Compos. Pt. A-Appl. Sci. Manuf.*, 2008, **39**, 1638-1643.
65. I. G. Campbell, T. A. Jones, W. D. Foulkes and J. Trowsdale, *Cancer Res.*, 1991, **51**, 5329-5338.
66. J. F. Ross, P. K. Chaudhuri and M. Ratnam, *Cancer*, 1994, **73**, 2432-2443.
67. X. Y. Shi, S. H. Wang, I. Lee, M. W. Shen and J. R. Baker, Jr., *Biopolymers*, 2009, **91**, 936-942.

Figure captions

Scheme 1. Schematic representation of the synthesis of functionalized dendrimers (a) and the formation of dendrimer-functionalized CA nanofibers for cancer cell capture applications (b).

Figure 1. ^{1}H NMR spectrum of G5.NH_2-FI-FA conjugate.

Figure 2. SEM micrograph and diameter distribution histogram of electrospun CA nanofibers.

Figure 3. FTIR spectra of (1) G5.NH_2 dendrimer, (2) CA nanofibers before hydrolysis, (3) CA nanofibers after hydrolysis, (4) G5.NHAc-FI-modified CA nanofibers, and (5) G5.NHAc-FI-FA-modified CA nanofibers.

Figure 4. CLSM images of G5.NHAc-FI-FA-modified CA nanofibers. Left: phase contrast image. Middle: fluorescent image. Right: overlap of phase contrast image with fluorescent image.

Figure 5. SEM micrographs and diameter distribution histograms of (a) G5.NHAc-FI-FA- and (b) G5.NHAc-FI-modified CA nanofibers, respectively.

Figure 6. The KB-HFAR cell capture efficiency of G5.NHAc-FI- and G5.NHAc-FI-FA-modified CA nanofibrous mats at different time points.

Figure 7. CLSM images of KB-HFAR cells captured on (a) G5.NHAc-FI- and (b) G5.NHAc-FI-FA-modified CA nanofibrous mats at different time points.

Figure 8. The capture efficiency of L929 cells (a) and KB-LFAR cells (b) using G5.NHAc-FI- and G5.NHAc-FI-FA-modified CA nanofibrous mats at different time points.

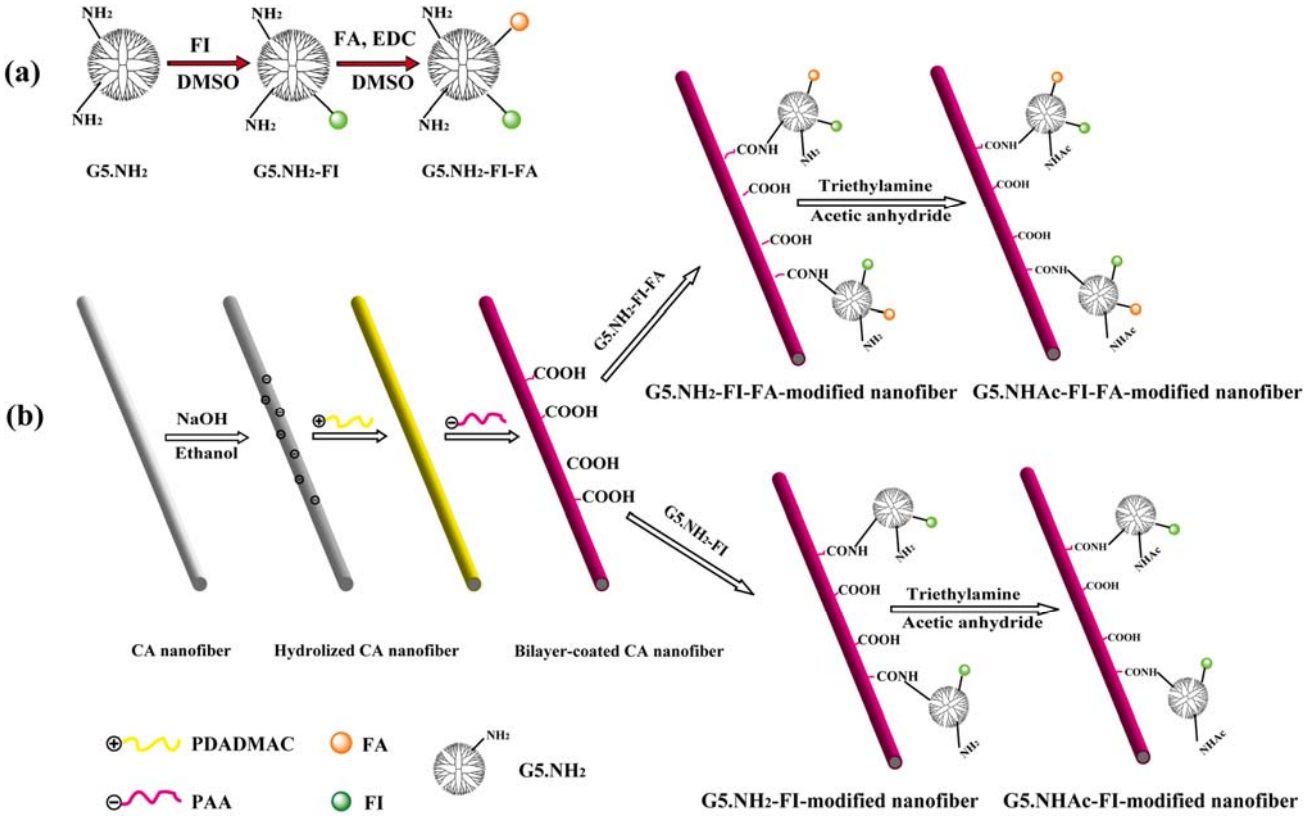

Scheme 1

Zhao *et al.*

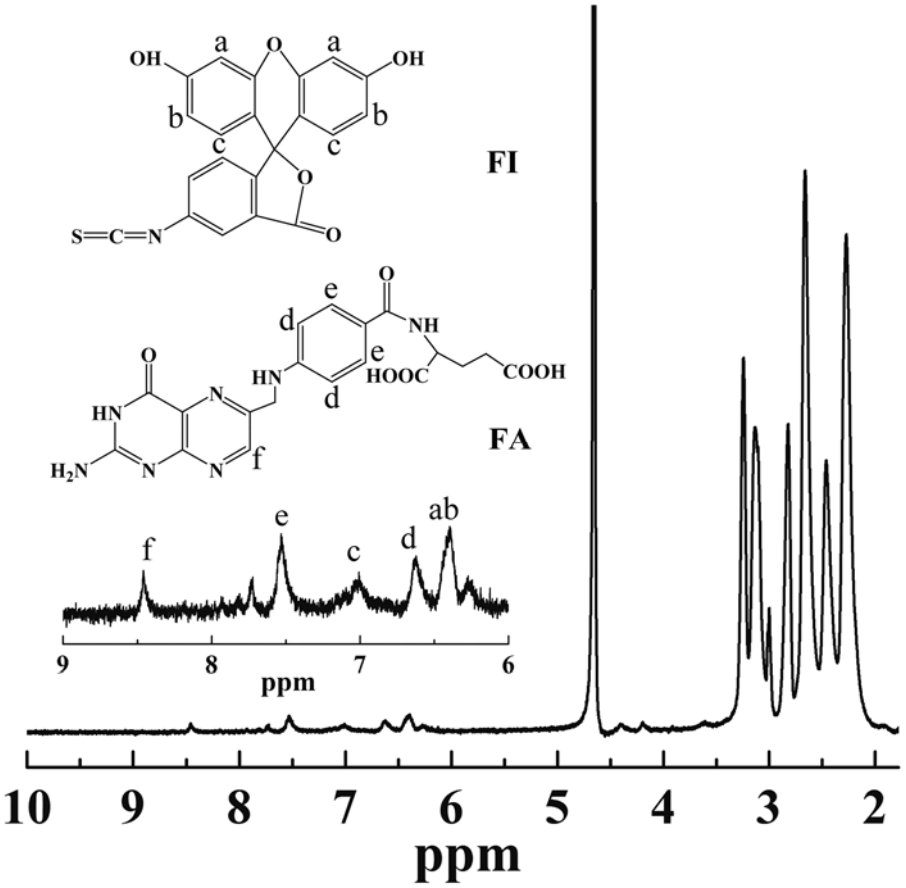

Figure 1

Zhao *et al.*

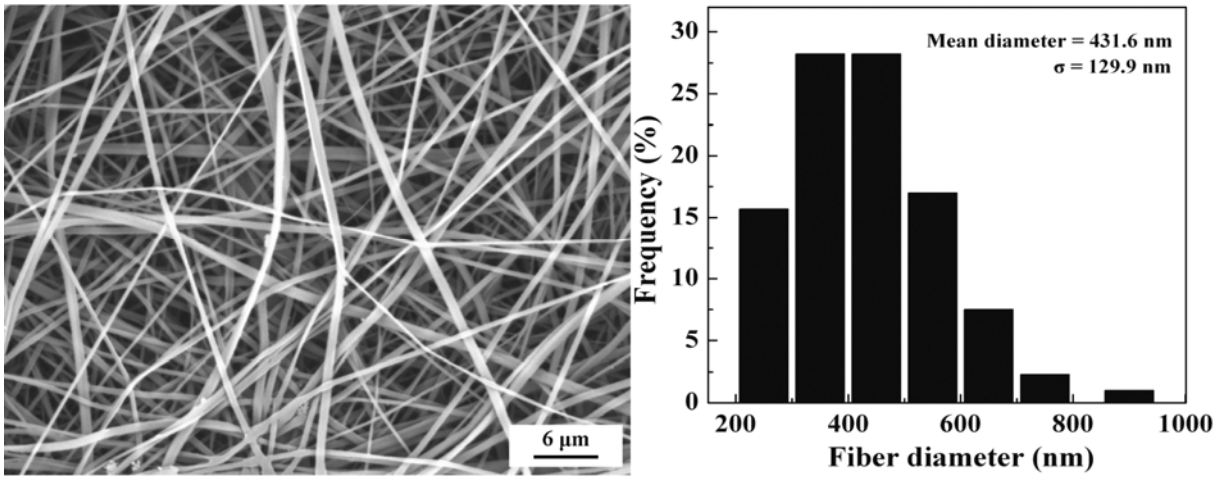

Figure 2

Zhao *et al*.

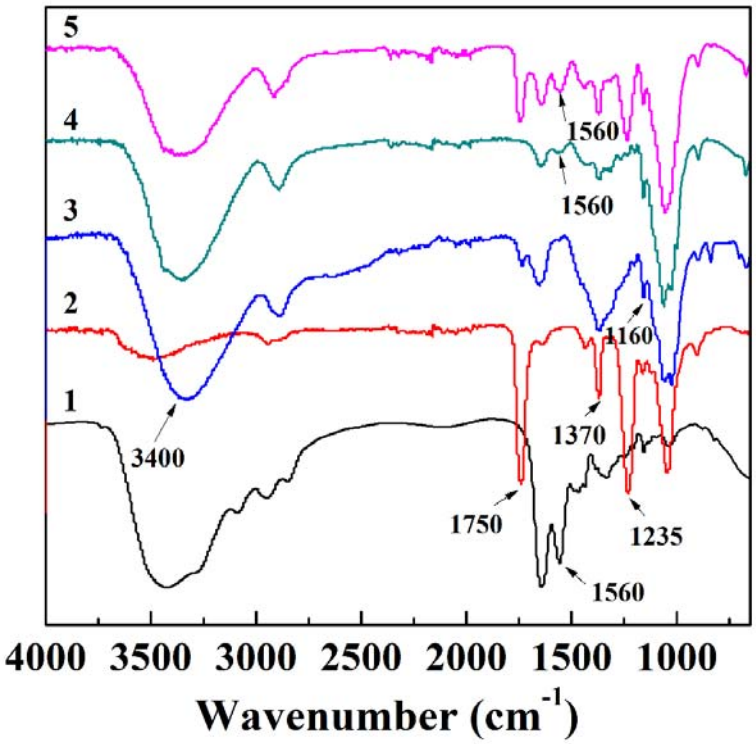

Figure 3

Zhao *et al*.

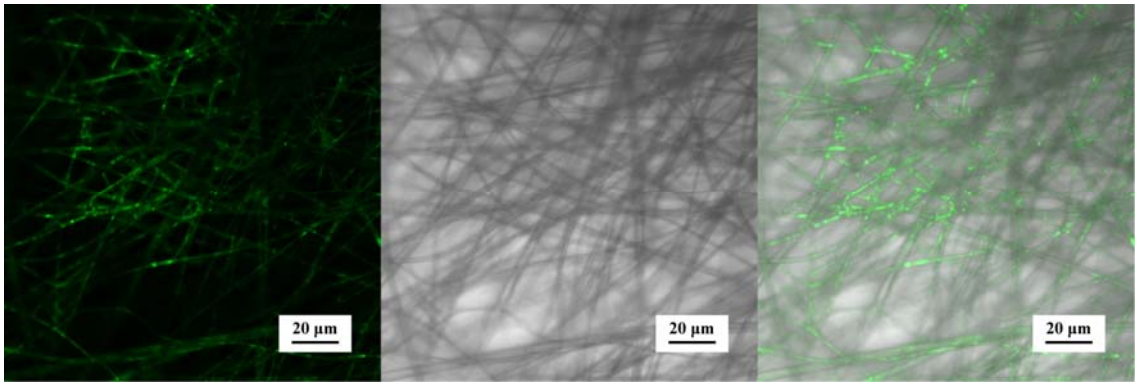

Figure 4

Zhao *et al.*

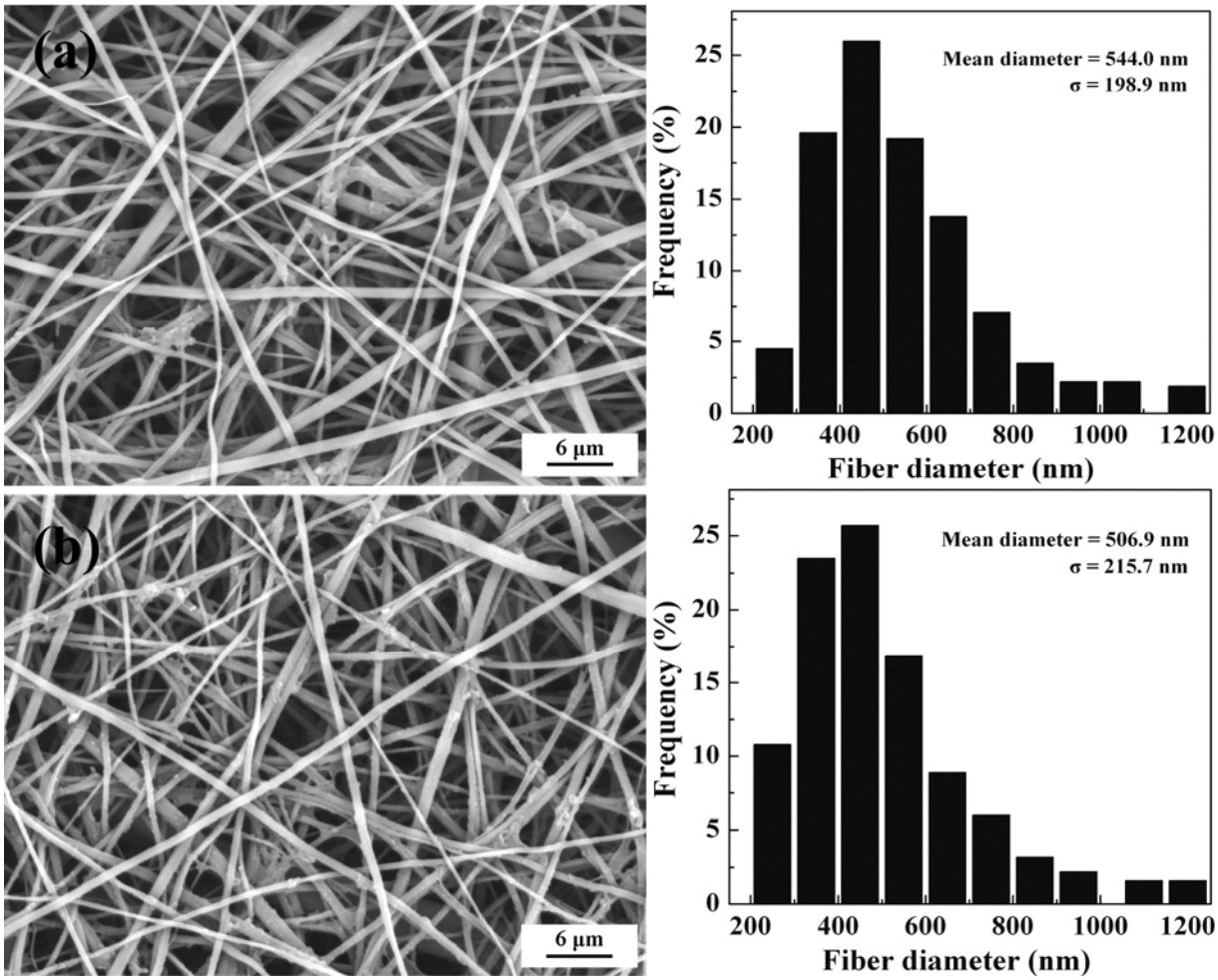

Figure 5

Zhao *et al.*

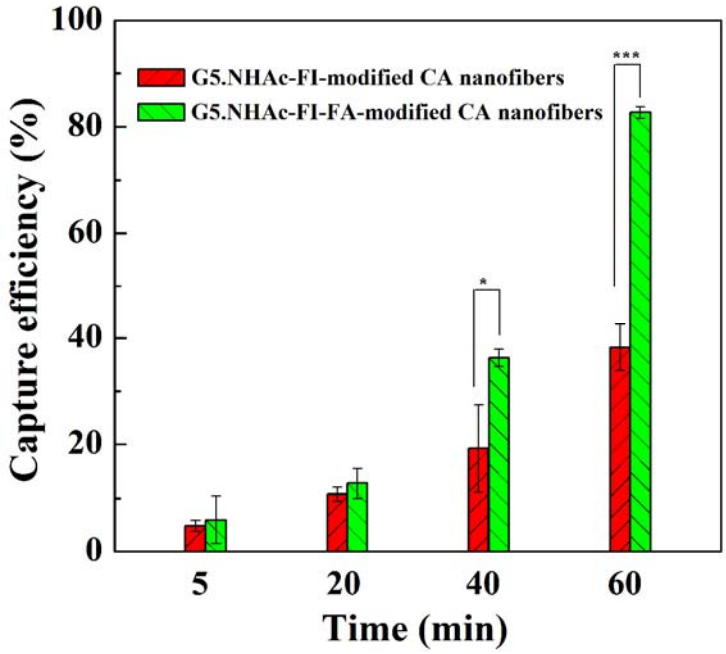

Figure 6

Zhao *et al*.

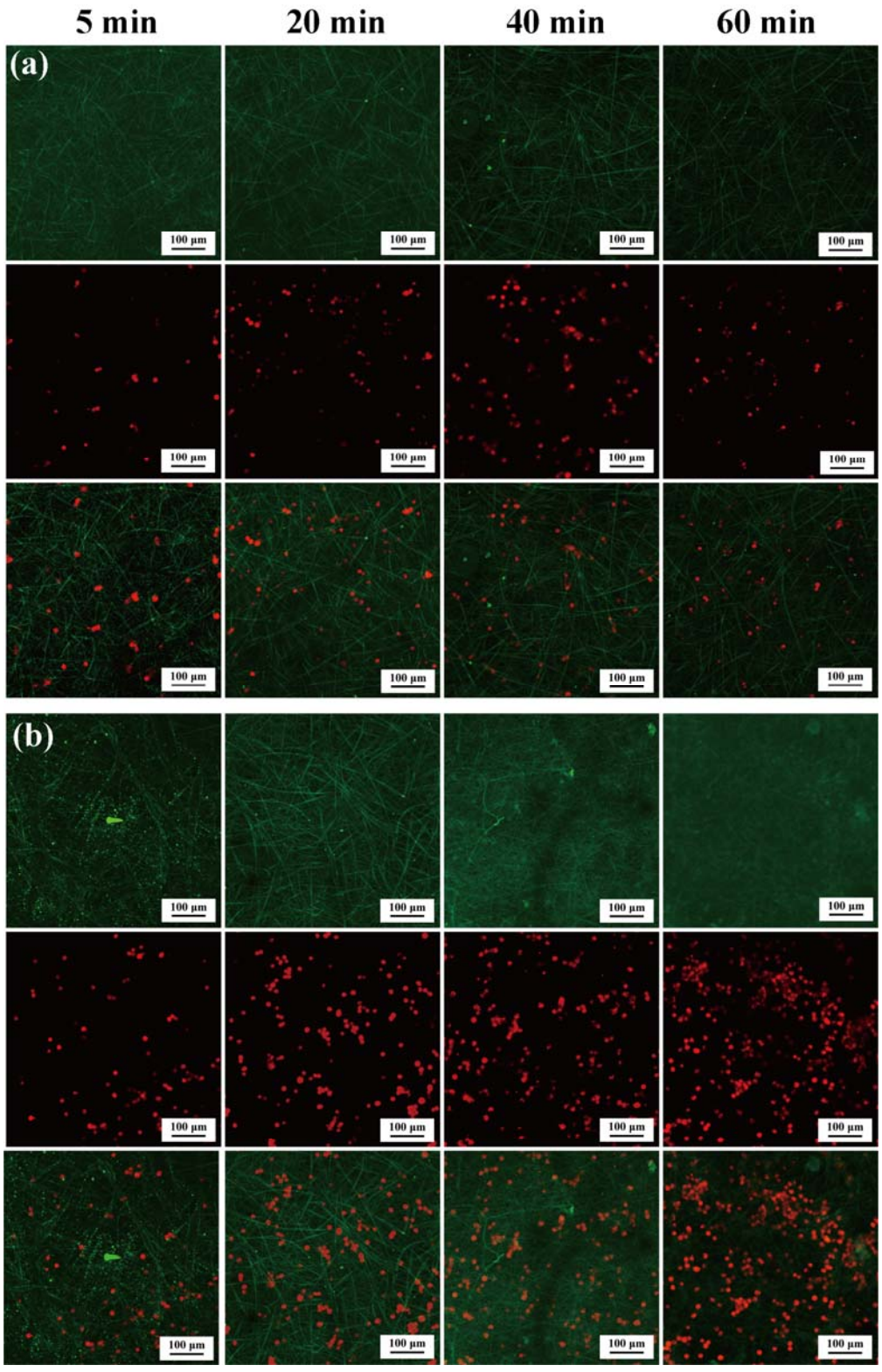

Figure 7

Zhao *et al.*

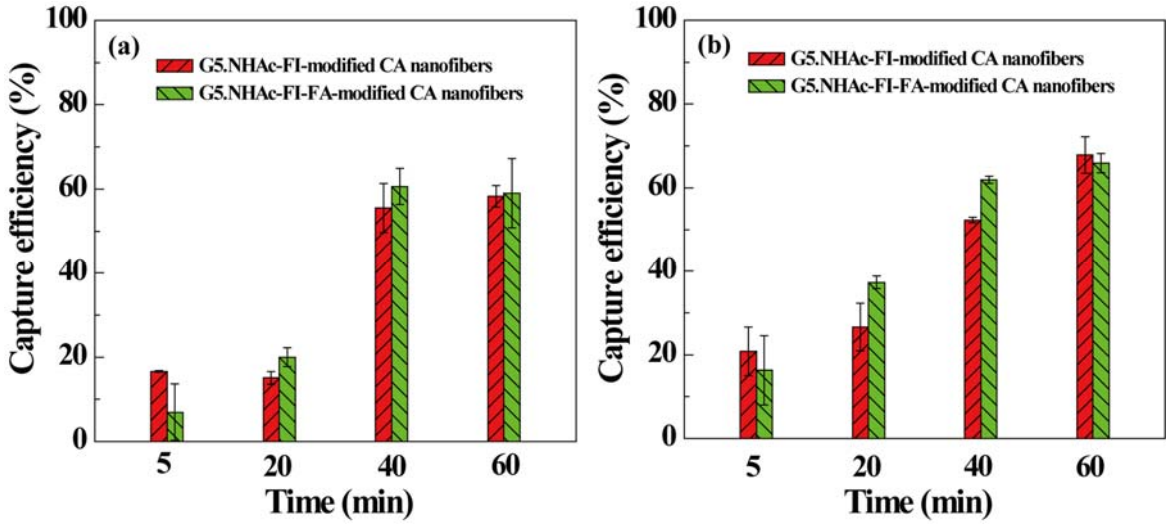

Figure 8

Zhao *et al*.